Journal of Geodesy (1998) 72: 304–312

Journal of Geodesy

Inverse Vening Meinesz formula and deflection-geoid formula: applications to the predictions of gravity and geoid over the South China Sea

C. Hwang

Department of Civil Engineering, National Chiao Tung University, 1001 Ta Hsueh Road, Hsinchu 30050, Taiwan, ROC
Fax: +886 3 5716257; e-mail: hwang@geodesy.cv.nctu.edu.tw

Received: 7 April 1997 / Accepted: 7 January 1998

Abstract. Using the spherical harmonic representations of the earth's disturbing potential and its functionals, we derive the inverse Vening Meinesz formula, which converts deflection of the vertical to gravity anomaly using the gradient of the H function. The deflection-geoid formula is also derived that converts deflection to geoidal undulation using the gradient of the C function. The two formulae are implemented by the 1D FFT and the 2D FFT methods. The innermost zone effect is derived. The inverse Vening Meinesz formula is employed to compute gravity anomalies and geoidal undulations over the South China Sea using deflections from Seasat, Geosat, ERS-1 and TOPEX//POSEIDON satellite altimetry. The 1D FFT yields the best result of 9.9-mgal rms difference with the shipborne gravity anomalies. Using the simulated deflections from EGM96, the deflection-geoid formula yields a 4-cm rms difference with the EGM96-generated geoid. The predicted gravity anomalies and geoidal undulations can be used to study the tectonic structure and the ocean circulations of the South China Sea.

Key words Deflection-geoid formula · Gravity anomaly · Inverse Vening Meinesz formula · Satellite altimetry · South China Sea

1 Introduction

Since the publication of the Vening Meinesz formula (Vening Meinesz 1928), little attention has been paid to its inverse formula, which converts deflections of the vertical to gravity anomalies. This is mainly because measurements of deflections are not widely available. With the advent of satellite altimetry, however, deflections of the vertical become available in the oceans and the inverse Vening Meinesz formula can be useful if one wishes to compute marine gravity from satellite altimetry. Marine deflections of the vertical can be derived from altimeter-measured geoidal undulations (if the sea-surface topography is properly removed) and the use of deflection as data type can reduce many systematic errors in satellite altimetry (Hwang 1997). Indeed, a frequency-domain version of the inverse Vening Meinesz formula exists in the literature, e.g., Haxby et al. (1983), Hwang and Parsons (1996), Sandwell and Smith (1997). A space-domain version has also been derived in, e.g., Molodenskii et al. (1962, Eq. III. 2.11). This paper attempts to derive the inverse Vening Meinesz formula for all cases using a spectral representation approach. The deflection-geoid formula, which converts deflections of the vertical to geoidal undulations, will be also derived using the same approach. Practical methods for implementing the two formulae will be presented. As an example, the two formulae will be employed to compute the gravity anomalies and the geoidal undulations over the South China Sea using the deflections of the vertical from Seasat, Geosat, ERS-1 and TOPEX/POSEIDON satellite altimetry.

2 Fundamentals

First we briefly review some of the basic equations in physical geodesy necessary for the derivations of the inverse Vening Meinesz formula and the deflection-geoid formula. The earth's disturbing potential T can be expanded into a series of spherical harmonics as

$$T(r,\phi,\lambda)=\frac{GM}{r}\sum_{n=2}^{\infty}\left(\frac{R}{r}\right)^{n}\sum_{m=0}^{n}\sum_{\alpha=0}^{1}C_{nm}^{\alpha}Y_{nm}^{\alpha}(\phi,\lambda) \tag{1}$$

where r,ϕ,λ are the spherical coordinates (geocentric distance, geocentric latitude and longitude), R is the earth's mean radius, C_{nm}^{α} are the harmonic coefficients and Y_{nm}^{α} are the fully normalized spherical harmonics defined as

$$Y_{nm}^{\alpha}(\phi,\lambda)=\begin{cases}\overline{R}_{nm}(\phi,\lambda)=\overline{P}_{nm}(\sin\phi)\cos m\lambda, \alpha=0\\ \overline{S}_{nm}(\phi,\lambda)=\overline{P}_{nm}(\sin\phi)\sin m\lambda, \alpha=1\end{cases} \tag{2}$$

with $\overline{P}_{nm}(\sin\phi)$ being the fully normalized associated Legendre function (Heiskanen and Moritz 1967). On the sphere of radius R, geoidal undulation can be expressed as

$$N(\phi,\lambda)=\frac{T}{\gamma_0}\,|_{r=R}=R\sum_{n=2}^{\infty}\sum_{m=0}^{n}\sum_{\alpha=0}^{1}C_{nm}^{\alpha}Y_{nm}^{\alpha}(\phi,\lambda) \tag{3}$$

and gravity anomaly as

$$\begin{aligned}\Delta g(\phi,\lambda)=&\left(-\frac{\partial T}{\partial r}-\frac{2}{r}T\right)|_{r=R}=\gamma_0\sum_{n=2}^{\infty}(n-1)\\&\times\sum_{m=0}^{n}\sum_{\alpha=0}^{1}C_{nm}^{\alpha}Y_{nm}^{\alpha}(\phi,\lambda)\end{aligned} \tag{4}$$

where

$$\gamma_0=\frac{GM}{R^2} \tag{5}$$

is the mean gravity. Spherical harmonic representations of other functionals of the earth's disturbing potential can be found in Rummel and van Gelderen (1995). Geoidal undulation and gravity anomaly are two scalar functions derived from the earth's disturbing potential. Deflection of the vertical, however, is a vector function and can be expressed as

$$\begin{aligned}\bar{z}(\phi,\lambda)=(\xi\ \eta)&=-\frac{1}{R}\nabla N(\phi,\lambda)\\&=-\sum_{n=2}^{\infty}\sum_{m=0}^{n}\sum_{\alpha=0}^{1}C_{nm}^{\alpha}\nabla Y_{nm}^{\alpha}(\phi,\lambda)\end{aligned} \tag{6}$$

where ξ and η are the north-south component and west-east component of the deflection vector, respectively, and ∇ is the gradient operator on the sphere defined as:

$$\nabla=\left(\frac{\partial}{\partial\phi}\ \frac{\partial}{\cos\phi\partial\lambda}\right) \tag{7}$$

Thus the basis functions of the deflection vector are ∇Y_{nm}^{α}, rather than Y_{nm}^{α}.

Finally we recall a variant of Green's formula (Meissl 1971, p. 12)

$$\iint_{\sigma}\nabla f\cdot\nabla g\,\mathrm{d}\sigma=-\iint_{\sigma}f\Delta^{*}g\,\mathrm{d}\sigma=-\iint_{\sigma}g\Delta^{*}f\,\mathrm{d}\sigma \tag{8}$$

where f and g are two arbitrary functions defined on the unit sphere, and Δ^{*} is the Laplace surface operator (Courant and Hilbert 1953) defined as

$$\Delta^{*}=\frac{1}{\cos\phi}\left[\frac{\partial}{\partial\phi}\left(\cos\phi\frac{\partial}{\partial\phi}\right)+\frac{1}{\cos^2\phi}\frac{\partial^2}{\partial\lambda^2}\right] \tag{9}$$

For the surface spherical harmonics, we have

$$\Delta^{*}Y_{nm}^{\alpha}(\phi,\lambda)+n(n+1)Y_{nm}^{\alpha}(\phi,\lambda)=0 \tag{10}$$

Using Eqs. (8) and (10) and the orthogonality relationship of fully normalized spherical harmonics (Heiskanen and Moritz 1967, p. 31), we obtain the result

$$\begin{aligned}&\iint_{\sigma}\nabla Y_{nm}^{\alpha}\cdot\nabla Y_{sr}^{\beta}\,\mathrm{d}\sigma\\&=\begin{cases}4\pi n(n+1), & \text{if } n=s \text{ and } m=r \text{ and } \alpha=\beta\\ 0, & \text{if } n\neq s \text{ or } m\neq r \text{ or } \alpha\neq\beta\end{cases}\end{aligned} \tag{11}$$

3 The inverse Vening Meinesz formula

The key to deriving the inverse Vening Meinesz formula is to look for a suitable kernel function for converting deflection of the vertical to gravity anomaly. Based on Meissl's (1971) approach, we introduce the kernel function H defined as

$$H(\psi_{pq})=\sum_{n=2}^{\infty}\frac{(2n+1)(n-1)}{n(n+1)}P_n(\cos\psi_{pq}) \tag{12}$$

where p and q are two points on the unit sphere with a spherical separation of ψ_{pq}, so that (see Fig. 1)

$$\cos\psi_{pq}=\sin\phi_p\sin\phi_q+\cos\phi_p\cos\phi_q\cos(\lambda_q-\lambda_p) \tag{13}$$

The Legendre polynomial $P_n\ (\cos\psi_{pq})$ in Eq. (12) can be further decomposed into the series:

$$P_n(\cos\psi_{pq})=\frac{1}{2n+1}\sum_{m=0}^{n}\sum_{\alpha=0}^{1}Y_{nm}^{\alpha}(\phi_p,\lambda_p)Y_{nm}^{\alpha}(\phi_q,\lambda_q) \tag{14}$$

which is termed decomposition formula by Heiskanen and Moritz (1967), see also Hobson (1965). Integrating the scalar products of ∇H and ∇N over the unit sphere and using Eq. (11), we get

$$\begin{aligned}&\iint_{\sigma}\nabla_q H(\psi_{pq})\cdot\nabla_q N(q)\mathrm{d}\sigma_q\\&=R\iint_{\sigma}\left[\sum_{n=2}^{\infty}\frac{n-1}{n(n+1)}\sum_{m=0}^{n}\sum_{\alpha=0}^{1}Y_{nm}^{\alpha}(p)\nabla_q Y_{nm}^{\alpha}(q)\right]\\&\quad\times\left[\sum_{n=2}^{\infty}\sum_{m=0}^{n}\sum_{\alpha=0}^{1}C_{nm}^{\alpha}\nabla_q Y_{nm}^{\alpha}(q)\right]\mathrm{d}\sigma_q\\&=R\sum_{n=2}^{\infty}\frac{n-1}{n(n+1)}\sum_{m=0}^{n}\sum_{\alpha=0}^{1}C_{nm}^{\alpha}Y_{nm}^{\alpha}(p)\\&\quad\times\iint_{\sigma}\left[\nabla_q Y_{nm}^{\alpha}(q)\cdot\nabla_q Y_{nm}^{\alpha}(q)\right]\mathrm{d}\sigma_q\\&=4\pi R\sum_{n=2}^{\infty}(n-1)\sum_{m=0}^{n}\sum_{\alpha=0}^{1}C_{nm}^{\alpha}Y_{nm}^{\alpha}(p)\end{aligned} \tag{15}$$

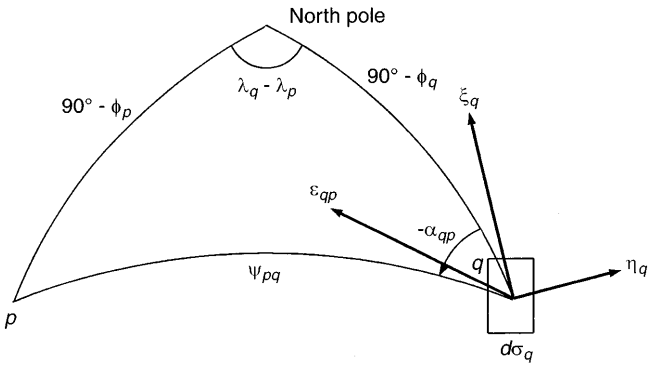

Fig. 1. Spherical distance ψ_{pq} between points p and q, and components of the deflection of the vertical at q

Comparing Eqs. (4) and (15), we have

$$\Delta g(p) = \frac{\gamma_0}{4\pi R} \iint_\sigma \nabla_q H(\psi_{pq}) \cdot \nabla_q N(q) \mathrm{d}\sigma_q \tag{16}$$

As shown in the Appendix, the closed form of H is

$$H(\psi_{pq}) = \frac{1}{\sin\frac{\psi_{pq}}{2}} + \log\left(\frac{\sin^3\frac{\psi_{pq}}{2}}{1+\sin\frac{\psi_{pq}}{2}}\right) \tag{17}$$

Furthermore,

$$\nabla_q H(\psi_{pq}) = \frac{\mathrm{d}H}{\mathrm{d}\psi_{pq}} \nabla_q \psi_{pq} = \frac{\mathrm{d}H}{\mathrm{d}\psi_{pq}} \left(\frac{\partial\psi_{pq}}{\partial\phi_q} \frac{\partial\psi_{pq}}{\cos\phi_q \partial\lambda_q}\right) \tag{18}$$

With Eq. (17) the derivative of H with respect to ψ_{pq} is

$$H' = \frac{\mathrm{d}H}{\mathrm{d}\psi_{pq}} = -\frac{\cos\frac{\psi_{pq}}{2}}{2\sin^2\frac{\psi_{pq}}{2}} + \frac{\cos\frac{\psi_{pq}}{2}(3+2\sin\frac{\psi_{pq}}{2})}{2\sin\frac{\psi_{pq}}{2}(1+\sin\frac{\psi_{pq}}{2})} \tag{19}$$

Differentiating Eq. (13) with respect to ϕ_q and λ_q, we have (cf. Heiskanen and Moritz 1967, p. 113)

$$\begin{aligned} -\sin\psi_{pq}\frac{\partial\psi_{pq}}{\partial\phi_q} &= \cos\phi_q\sin\phi_p - \sin\phi_q\cos\phi_p\cos(\lambda_q-\lambda_p) \\ -\sin\psi_{pq}\frac{\partial\psi_{pq}}{\partial\lambda_q} &= -\cos\phi_p\cos\phi_q\sin(\lambda_q-\lambda_p) \end{aligned} \tag{20}$$

Referring to the spherical triangle in Fig. 1, the following relationships hold:

$$\begin{aligned} \sin\psi_{pq}\cos\alpha_{qp} &= \cos\phi_q\sin\phi_p - \sin\phi_q\cos\phi_p\cos(\lambda_q-\lambda_p) \\ \sin\psi_{pq}\sin\alpha_{qp} &= -\cos\phi_p\sin(\lambda_q-\lambda_p) \end{aligned} \tag{21}$$

Thus

$$\frac{\partial\psi_{pq}}{\partial\phi_q} = -\cos\alpha_{qp}, \frac{\partial\psi_{pq}}{\partial\lambda_q} = -\cos\phi_q\sin\alpha_{qp} \tag{22}$$

Inserting Eqs. (18) and (22) into Eq. (16) we finally get the *inverse Vening Meinesz formula*

$$\begin{aligned} \Delta g(p) &= -\frac{\gamma_0}{4\pi}\iint_\sigma H'\left(\frac{\partial\psi_{pq}}{\partial\phi_q}\frac{\partial\psi_{pq}}{\cos\phi\partial\lambda_q}\right)\cdot(\xi_q\eta_q)\mathrm{d}\sigma_q \\ &= \frac{\gamma_0}{4\pi}\iint_\sigma H'(\xi_q\cos\alpha_{qp}+\eta_q\sin\alpha_{qp})\mathrm{d}\sigma_q \\ &= \frac{\gamma_0}{4\pi}\iint_\sigma H'\varepsilon_{qp}\mathrm{d}\sigma_q \end{aligned} \tag{23}$$

where ε_{qp} is the deflection component at point q in the direction of the azimuth α_{qp} (Heiskanen and Moritz 1967, p. 187), or simply the longitudinal deflection component. The meaning of the inverse Vening Meinesz formula is: assuming that everywhere on the unit sphere the north-south and west-east deflection components are known, the gravity anomaly at any given point can be obtained by integrating the products of H' and the longitudinal deflection components over the unit sphere.

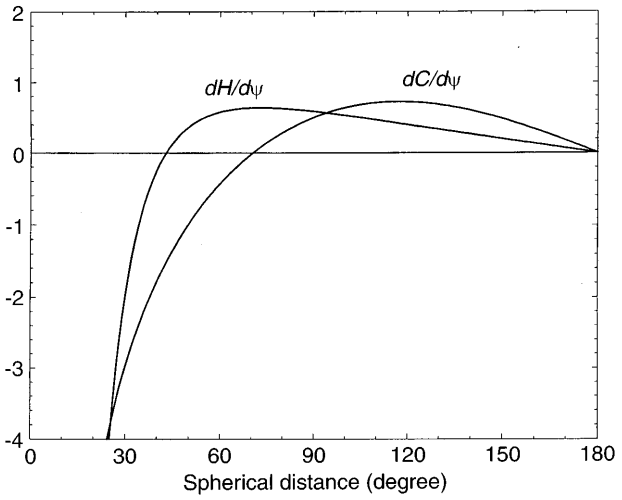

Fig. 2. Function $H'(\psi)$ and function $C'(\psi)$

Figure 2 shows the function H', which changes rapidly as ψ approaches zero. The first zero crossing of H' occurs at $\psi = 43°$. When ψ is small, we have the asymptotic representation:

$$H'(\psi) \approx -\frac{2}{\psi^2} \tag{24}$$

It is noted that the asymptotic representation of H' is equal to that of $\mathrm{d}S/\mathrm{d}\psi$ (the derivative of Stokes' function) and agrees with the asymptotic representation of the kernel function in Eq. (III.2.111) of Molodenskii et al. (1962). Furthermore, $H(\psi) \approx \frac{2}{\psi}$ as ψ approaches zero, so the asymptotic representations of the function H and Stokes' function are identical.

4 The deflection-geoid formula

Next we derive a formula for converting deflection of the vertical to geoidal undulation. The derivation is almost the same as that for the inverse Vening Meinesz formula. First, we introduce the kernel function C

$$C(\psi_{pq}) = \sum_{n=2}^{\infty}\frac{2n+1}{n(n+1)}P_n(\cos\psi_{pq}) \tag{25}$$

Then,

$$\begin{aligned} &\iint_\sigma \nabla_q C(\psi_{pq})\cdot\nabla_q N(q)\mathrm{d}\sigma_q \\ &= R\iint_\sigma\left[\sum_{n=2}^{\infty}\frac{1}{n(n+1)}\sum_{m=0}^{n}\sum_{\alpha=0}^{1}Y_{nm}^{\alpha}(p)\nabla_q Y_{nm}^{\alpha}(q)\right] \\ &\quad\times\left[\sum_{n=2}^{\infty}\sum_{m=0}^{n}\sum_{\alpha=0}^{1}C_{nm}^{\alpha}\nabla_q Y_{nm}^{\alpha}(q)\right]\mathrm{d}\sigma_q \end{aligned}$$

$$= R\sum_{n=2}^{\infty}\frac{1}{n(n+1)}\sum_{m=0}^{n}\sum_{\alpha=0}^{1}C_{nm}^{\alpha}Y_{nm}^{\alpha}(p)$$
$$\times\iint_{\sigma}[\nabla_q Y_{nm}^{\alpha}(q)\cdot\nabla_q Y_{nm}^{\alpha}(q)]\mathrm{d}\sigma_q \quad (26)$$
$$= 4\pi R\sum_{n=2}^{\infty}\sum_{m=0}^{n}\sum_{\alpha=0}^{1}C_{nm}^{\alpha}Y_{nm}^{\alpha}(p)$$

Thus, the geoidal undulation at point p can be obtained by integrating the scalar products of ∇H and ∇N over the unit sphere:

$$N(p)=\frac{1}{4\pi}\iint_{\sigma}\nabla_q H(\psi_{pq})\cdot\nabla_q N(q)\mathrm{d}\sigma_q \quad (27)$$

Using Eqs. (22) and (27) we obtain the *deflection-geoid formula*

$$N(p)=\frac{R}{4\pi}\iint_{\sigma}\frac{\mathrm{d}C}{\mathrm{d}\psi_{pq}}\varepsilon_{qp}\mathrm{d}\sigma_q \quad (28)$$

According to the Appendix, the closed form of C is

$$C(\psi_{pq})=-2\log\sin\frac{\psi_{pq}}{2}-\frac{3}{2}\cos\psi_{pq}-1 \quad (29)$$

and

$$C'=\frac{\mathrm{d}C}{\mathrm{d}\psi_{pq}}=-\cot\frac{\psi_{pq}}{2}+\frac{3}{2}\sin\psi_{pq} \quad (30)$$

which agrees with the result of Molodenskii et al. (1962, Eq. III.2.8) if the summation of the series in Eq. (25) starts from $n=1$. Figure 2 also shows the funciton C'. The first zero crossing of C' occurs at $\psi=70.5°$. The asymptotic representation of C' when ψ is small is:

$$C'(\psi)\approx-\frac{2}{\psi} \quad (31)$$

5 Computations by 1D FFT: rigorous implementations

We propose two computational schemes for the inverse Vening Meinesz formula and the deflection-geoid formula when the north-south and west-east components of deflections are given on a regular grid. The first scheme is based on the one-dimensional fast Fourier transform (1D FFT) method, which, given regularly gridded data, can rigorously implement a surface integral such as Eq. (23) or (28). In such a scheme, gravity anomalies or geoidal undulations at the same parallel are computed simultaneously by FFT as (cf. Haagmans et al. 1993)

$$\begin{Bmatrix}\Delta g_{\phi_p}(\lambda_p)\\ N_{\phi_p}(\lambda_p)\end{Bmatrix}=\begin{Bmatrix}\gamma_0\\ R\end{Bmatrix}\frac{\Delta\phi\Delta\lambda}{4\pi}\sum_{\phi_q=\phi_1}^{\phi_n}\sum_{\lambda_q=\lambda_1}^{\lambda_n}\begin{Bmatrix}H'(\Delta\lambda_{qp})\\ C'(\Delta\lambda_{qp})\end{Bmatrix}$$
$$\times(\xi_{\cos}\cos\alpha_{qp}+\eta_{\cos}\sin\alpha_{qp})$$
$$=\begin{Bmatrix}\gamma_0\\ R\end{Bmatrix}\frac{\Delta\phi\Delta\lambda}{4\pi}\mathbf{F}_1^{-1}$$
$$\times\left\{\sum_{\phi_q=\phi_1}^{\phi_n}\begin{bmatrix}\mathbf{F}_1(H'(\Delta\lambda_{qp})\cos\alpha_{qp})\\ \mathbf{F}_1(C'(\Delta\lambda_{qp})\cos\alpha_{qp})\end{bmatrix}\right]\mathbf{F}_1(\xi_{\cos})$$
$$+\begin{bmatrix}\mathbf{F}_1(H'(\Delta\lambda_{qp})\sin\alpha_{qp})\\ \mathbf{F}_1(C'(\Delta\lambda_{qp})\sin\alpha_{qp})\end{bmatrix}]\mathbf{F}_1(\eta_{\cos})\Bigg\}$$

where $\xi_{\cos}=\xi\cos\phi,\eta_{\cos}=\eta\cos\phi,\Delta\lambda_{qp}=\lambda_q-\lambda_p,\Delta\phi$ and $\Delta\lambda$ are grid intervals in the directions of latitude and longitude, and $\mathbf{F}_1$ is the 1D FFT. Since all quantities are real-valued, we can compute the Fourier transforms of two real-valued arrays simultaneously to save computer time (Hwang 1993). Specifically, let $h(k)$ and $g(k)$, $k=0,\ldots,n-1$, be the two real-valued arrays to be Fourier transformed. We first form the complex array $y(k)$ as

$$y(k)=h(k)+i\,g(k),k=0,\ldots,n-1 \quad (33)$$

where $i=\sqrt{-1}$. Let $Y(k)$ be the Fourier transform of $y(k)$, we have

$$\begin{aligned}H(0)&=\mathrm{Re}(Y(0)),\ \text{and}\ H(k)=\tfrac{1}{2}\,\mathrm{Re}\,(Y(k)\\&\quad+Y(n-k))+\tfrac{1}{2}i\,\mathrm{Im}\,(Y(k)+Y(n-k))\\&\quad\text{for}\ \ k=1,\ldots,n-1\\G(0)&=\ \mathrm{Im}\,(Y(0)),\ \text{and}\ G(k)=\tfrac{1}{2}\,\mathrm{Re}\,(Y(k)\\&\quad+Y(n-k))-\tfrac{1}{2}i\,\mathrm{Im}\,(Y(k)+Y(n-k))\,\text{for}\\&\quad k=1,\ldots,n-1\end{aligned} \quad (34)$$

where $H(k)$ and $G(k)$ are the Fourier transforms of $h(k)$ and $g(k)$, respectively, and Re(.) and Im(.) are the real and the imaginary parts of a complex number. In practice, the complex array holding $\xi_{\cos}$ and $\eta_{\cos}$, and the complex array holding $H'(\Delta\lambda_{qp})\cos\alpha_{qp}$ and $H'(\Delta\lambda_{qp})\sin\alpha_{qp}$ (or $C'(\Delta\lambda_{qp})\cos\alpha_{qp}$ and $C'(\Delta\lambda_{qp})\sin\alpha_{qp}$) are Fourier transformed. Taking advantage of the gridded data, azimuth and spherical distance can be calculated as

$$\tan\alpha_{qp}=\frac{-\cos\phi_p\sin\Delta\lambda_{qp}}{-\sin(\phi_q-\phi_p)+2\sin\phi_q\cos\phi_p\sin^2\frac{\Delta\lambda_{qp}}{2}} \quad (35)$$

$$\sin^2\left(\frac{\psi_{qp}}{2}\right)=\sin^2\left(\frac{\Delta\phi_{qp}}{2}\right)+\sin^2\left(\frac{\Delta\lambda_{qp}}{2}\right)\cos\phi_q\cos\phi_p \quad (36)$$

where $\Delta\phi_{qp}=\phi_q-\phi_p$.

6 Computations by 2D FFT: planar approximations

The second computational scheme is based on the planar approximations of the two formulae, and hence the two-dimensional fast Fourier transform (2D FFT). In a local rectangular, $x-y$ coordinate system, the surface element and the spherical distance can be approximated as $R^2\mathrm{d}\sigma_q=\mathrm{d}x_q\mathrm{d}y_q$ and $\psi_{qp}=\frac{\rho_{qp}}{R}$, with ρ_{qp} being the planar distance. With the asymptotic representation in Eq. (24), the inverse Vening Meinesz formula becomes

$$\begin{aligned}\Delta g(x_p,y_p) &= \frac{\gamma_0}{4\pi}\iint_D \frac{-2R^2}{\rho_{qp}^3}\left[\xi_q(\rho_{qp}\cos\alpha_{qp})\right.\\ &\quad\left.+\eta_q(\rho_{qp}\sin\alpha_{qp})\right]\frac{\mathrm{d}x_q\mathrm{d}y_q}{R^2}\\ &= \frac{-\gamma_0}{2\pi}\left\{\iint_D \frac{y_p-y_q}{\left[(x_p-x_q)^2+(y_p-y_q)^2\right]^{\frac{3}{2}}}\xi_q\mathrm{d}x_q\mathrm{d}y_q\right.\\ &\quad\left.+\iint_D \frac{x_p-x_q}{\left[(x_p-x_q)^2+(y_p-y_q)^2\right]^{\frac{3}{2}}}\eta_q\mathrm{d}x_q\mathrm{d}y_q\right\}\\ &= \frac{-\gamma_0}{2\pi}\left\{\left(\frac{y}{(x^2+y^2)^{\frac{3}{2}}}\right)^*\xi+\left(\frac{x}{(x^2+y^2)^{\frac{3}{2}}}\right)^*\eta\right\}\end{aligned} \tag{37}$$

where * is the convolution operator and D is the data domain. Schwarz et al. (1990) show that

$$\mathbf{F}\left\{\begin{pmatrix}x\\y\end{pmatrix}(x^2+y^2)^{-3/2}\right\} = -2\pi i\begin{pmatrix}u\\v\end{pmatrix}(u^2+v^2)^{-3/2} \tag{38}$$

where $\mathbf{F}$ is the 2D FT, and u and v are the spatial frequencies. Thus the relationship between gravity anomaly and deflection components in the frequency domain is

$$\Delta\mathbf{G}(u,v) = \frac{i\gamma_0}{\sqrt{u^2+v^2}}[v\mathbf{X}(u,v)+u\mathbf{E}(u,v)] \tag{39}$$

where $\Delta\mathbf{G}, \mathbf{X}$ and $\mathbf{E}$ are the Fourier transforms of Δg, ξ, η, respectively. Equation (39) can also be found in, for example, Hwang and Parsons (1996), Sandwell and Smith (1997), Haxby et al. (1983), who derived this formula using different approaches.

The planar approximation of the deflection-geoid formula reads

$$\begin{aligned}N(x_p,y_p) &= \frac{R}{4\pi}\iint_D \frac{-2R}{\rho_{qp}^2}\left[\xi_q(\rho_{qp}\cos\alpha_{qp})\right.\\ &\quad\left.+\eta_q(\rho_{qp}\sin\alpha_{qp})\right]\frac{\mathrm{d}x_q\mathrm{d}y_q}{R^2}\\ &= \frac{-1}{2\pi}\left\{\iint_D \frac{y_p-y_q}{(x_p-x_q)^2+(y_p-y_q)^2}\xi_q\mathrm{d}x_q\mathrm{d}y_q\right.\\ &\quad\left.+\iint_D \frac{x_p-x_q}{(x_p-x_q)^2+(y_p-y_q)^2}\eta_q\mathrm{d}x_q\mathrm{d}y_q\right\}\\ &= \frac{-1}{2\pi}\left\{\left(\frac{y}{x^2+y^2}\right)^*\xi+\left(\frac{x}{x^2+y^2}\right)^*\eta\right\}\end{aligned} \tag{40}$$

The Fourier transforms of $\frac{x}{x^2+y^2}$ and $\frac{y}{x^2+y^2}$, which do not exist in the literature, are now derived. We begin with the definite integral found in Gradshteyn and Ryzhik (1994, p. 782):

$$\begin{aligned}&\int_0^\infty [\log(1+\sqrt{a^2+r^2})-\log r]J_0(br)r\mathrm{d}r\\ &= \frac{1}{b^2}(1-\mathrm{e}^{-ab}),\quad a>0,\quad b>0\end{aligned} \tag{41}$$

Let a in Eq. (41) approach infinity so that $1+\sqrt{a^2+r^2}=K$ remains a constant for any r, and $\mathrm{e}^{-ab}=0$. Then,

$$\int_0^\infty \log\left(\frac{K}{r}\right)J_0(br)r\mathrm{d}r = \frac{1}{b^2} \tag{42}$$

This means that the Hankel transform of $\log(\frac{K}{r})$ is $\frac{1}{2\pi q^2}$, with $q^2=u^2+v^2$. Furthermore,

$$\begin{pmatrix}x\\y\end{pmatrix}\frac{1}{x^2+y^2} = \begin{pmatrix}x\\y\end{pmatrix}\frac{1}{r^2} = -\begin{pmatrix}\frac{\partial}{\partial x}\\ \frac{\partial}{\partial y}\end{pmatrix}\log\left(\frac{K}{r}\right) \tag{43}$$

By the differentiation theorem of Fourier transform (see, e.g., Mesko 1984), we have

$$\mathbf{F}\left\{\begin{pmatrix}x\\y\end{pmatrix}\frac{1}{x^2+y^2}\right\} = -\mathrm{i}\begin{pmatrix}u\\v\end{pmatrix}\frac{1}{u^2+v^2} \tag{44}$$

With Eqs. (40) and (44), we obtain the relationship between geoidal undulation and deflection components in the frequency domain

$$\mathbf{N}(u,v) = \frac{\mathrm{i}}{2\pi(u^2+v^2)}[v\mathbf{X}(u,v)+u\mathbf{E}(u,v)] \tag{45}$$

which can also be found in Olgiati et al. (1995, Eq. 6). Using Eq. (39) and the geoid-gravity spectral relationship [see, e.g., Schwarz et al. (1990)], one can also derive Eq. (45).

7 The innermost zone effects

At zero spherical distance the kernel function H' and C' become singular and the azimuth is undefined. Thus we must account for the innermost zone effect (Heiskanen and Moritz 1967). First we consider such an effect in the inverse Vening Meinesz formula. The deflection components at the neighbourhood of point p can be expanded into the Taylor series (see Fig. 3)

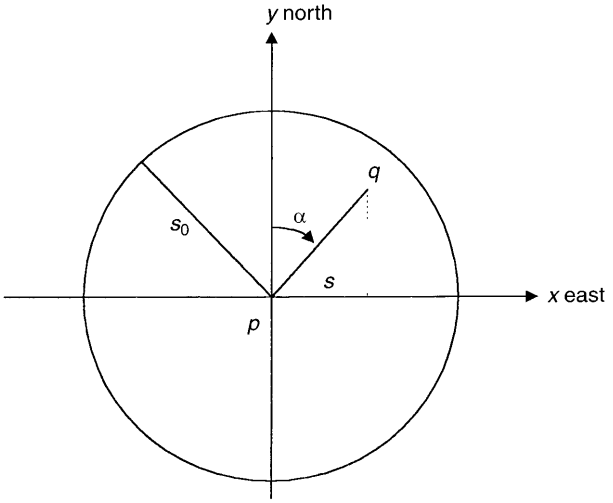

Fig. 3. Local rectangular coordinates for the innermost zone effect in a cap of radius s_0

$$\xi_q = \xi_p + x\xi_x + y\xi_y + \tfrac{1}{2}\left(x^2\xi_{xx} + 2xy\xi_{xy} + y^2\xi_{yy}\right) + \cdots$$
$$\eta_q = \eta_p + x\eta_x + y\eta_y + \tfrac{1}{2}\left(x^2\eta_{xx} + 2xy\eta_{xy} + y^2\eta_{yy}\right) + \cdots \quad (46)$$

where $\xi_x = \frac{\partial\xi}{\partial x}$, $\xi_y = \frac{\partial\xi}{\partial y}$, $\xi_{xx} = \frac{\partial^2\xi}{\partial x^2}$, $\xi_{yy} = \frac{\partial^2\xi}{\partial y^2}$ and $\xi_{xy} = \frac{\partial^2\xi}{\partial x\partial y}$. Retaining only the linear terms in Eq. (46) and assuming that the innermost zone is circular, with Eq. (24) we have

$$\begin{aligned}\Delta g_i &= \frac{\gamma_0}{4\pi}\int_{\alpha=0}^{2\pi}\int_{s=0}^{s0}\frac{-2}{s^2}[(\xi_p + s\,\sin\alpha\,\xi_x + s\,\cos\alpha\,\xi_y)\\ &\quad\times\cos(\alpha+\pi) + (\eta_p + s\,\sin\alpha\,\eta_x + s\,\cos\alpha\,\eta_y)\\ &\quad\times\sin(\alpha+\pi)]s\mathrm{d}s\mathrm{d}\alpha\\ &= \frac{\gamma_0}{2\pi}\left(\xi_y\int_{\alpha=0}^{2\pi}\cos^2\alpha\mathrm{d}\alpha\int_{s=0}^{s0}\mathrm{d}s\right.\\ &\quad\left.+\eta_x\int_{\alpha=0}^{2\pi}\sin^2\alpha\mathrm{d}\alpha\int_{s=0}^{s0}\mathrm{d}s\right)\\ &= \frac{s_0\gamma_0}{2}(\xi_y + \eta_x)\end{aligned} \quad (47)$$

Using a similar derivation, the innermost zone effect in the case of the deflection-geoid formula is

$$N_i = \frac{s_0^2}{4}(\xi_y + \eta_x) \quad (48)$$

Thus the innermost zone effects for gravity anomaly and geoidal undulation depend on the gradients of the deflection components. For discrete data ξ_y and η_x can be obtained by numerically differentiating ξ and η along the y and x directions, respectively. If the planar grid intervals are Δx and Δy, the radius of the innermost zone may be approximated by

$$s_0 = \sqrt{\frac{\Delta x\Delta y}{\pi}} \quad (49)$$

8 Applications: gravity and geoid over the South China Sea from satellite altimetry

As an application of the inverse Vening Meinesz formula, we computed marine gravity anomalies over the South China Sea (defined domain: $5^\circ \le$ latitude $\le 25^\circ$, $105^\circ \le$ longitude $\le 125^\circ$) using the 1D FFT and 2D FFT methods and the remove-restore procedure. The EGM96 geopotential model (Lemoine et al. 1997) to degree 360 was used as the reference field. The altimeter data used are from Seasat, Geosat/ERM, Geosat/GM, ERS-1/35-day, ERS-1/GM and TOPEX/POSEIDON. The sea-surface topography of Levitus (1982) is subtracted from the altimeter sea surface heights before generating the deflections of the vertical. At the centre of the South China Sea the average altimeter data density is 1560 points in $1^\circ \times 1^\circ$, and at the continental borders the densities drop sharply. We used the method of least-squares collocation and the covariance functions of deflections derived by Hwang and Parsons (1995) to grid the deflections of different azimuths into the north-south and west-east components at a $2' \times 2'$ interval. We used a 1°-border to avoid bad results at the edges. Further, 100% zero paddings were applied to data arrays and kernel arrays to avoid edge effects in convolutions by FFT. Table 1 shows the comparisons between the shipborne gravity anomalies and the gravity anomalies derived from the 1D FFT, the 2D FFT, and Sandwell and Smith's (1997) methods. The shipborne gravity anomalies were provided by the National Geophysical Data Center (NGDC). A total of 180297 shipborne gravity anomalies were used for the comparisons. The 1D FFT produces a slightly better result than the 2D FFT. Table 1 also shows the CPU time ratio between a given method and the 2D FFT method on a Sun Sparc 20 machine. The 1D FFT requires more than doubled computer time than the 2D FFT. Employing the innermost zone effect improves the result. We also did tests in other areas, and found that the innermost zone effect always improves the result. Furthermore, the result from the 1D FFT is about 30% better than the recently published altimeter-derived gravity anomalies from Sandwell and Smith (1997). Figure 4 shows the predicted gravity anomalies over the South China Sea (1D FFT plus innermost zone effect). In Fig. 4, the outline of the basin of the South China Sea is clearly visible. A median valley-like feature running from the southwest to the northeast is probably the spreading centre of the South China Sea, which has been identified by, e.g., Briais et al. (1993), using geomagnetic data. The predicted gravity anomalies can be further used to interpret the tectonic structure of the South China Sea.

Table 1. RMS differences between the shipborne and the predicted gravity anomalies over the South China Sea and the CPU time ratios ([a]IE: innermost zone effect)

Method	RMS difference (mgal)	CPU time ratio
1D FFT/IE[a]	9.90	2.8
1D FFT/no IE	10.06	2.4
2D FFT	10.11	1.0
Sandwell and Smith (1997)	14.32	unavailable

Because generally there are no measured geoidal undulations at sea, we used the simulation approach of Tziavos (1996) to evaluate the performances of the 1D and 2D FFT methods that implement the deflection-geoid formula. First, over the South China Sea we generated gridded north-south and west-east components of deflections, and geoidal undulations using harmonic coefficients from EGM96 (Lemoine et al. 1997) at a $7.5' \times 7.5'$ interval. Only harmonic coefficients between degrees 181 and 360 were used, so that the remove-restore procedure need not be used. Because going from deflection to geoid is a smoothing process, we used a 5° border to avoid edge effects. The north-south and west-east deflection components were then used to compute geoidal undulations. The statis-

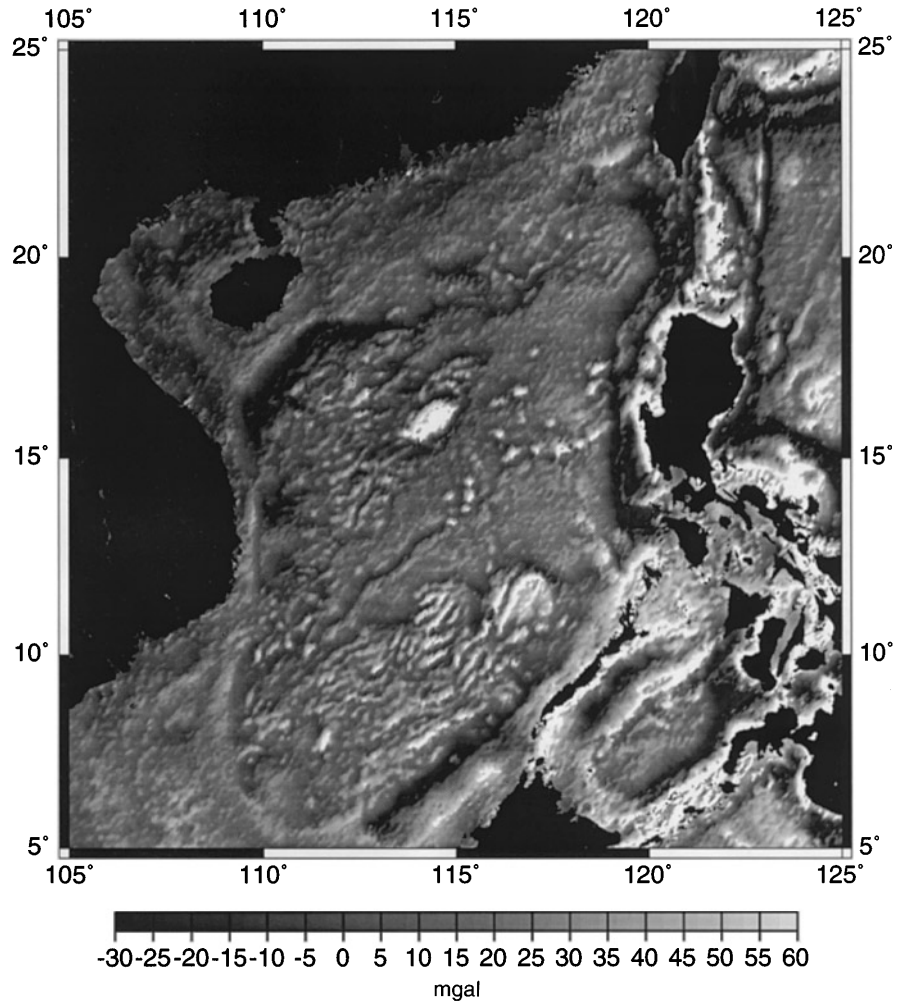

Fig. 4. Grey-shaded relief map of the predicted gravity anomalies over the South China Sea, with illumination from the north-west

tics of the differences between the EGM96-generated undulations, considered as the "ground truth", and the computed undulations from various methods are given in Table 2. From Table 2, the 1D FFT again gives a better result than the 2D FFT. Also, the use of the innermost zone effect significantly reduces the difference between the 'true' and the predicted geoids. Having done these tests, we then used the deflection data as used in predicting the gravity anomalies to compute the geoidal undulations over the South China Sea. The result is shown in Fig. 5. The predicted geoid can be used to study the ocean circulations over the South China Sea, which recently have received considerable attention from the oceanographers in Southeast Asia.

9 Conclusion

In this paper we showed the detailed derivations of the inverse Vening Meinesz formula and the deflection-geoid formula using the spherical harmonic representations of the functionals of the earth's disturbing potential, and for each we presented the 1D FFT and 2D FFT methods for computations. In all cases the 1D FFT yields better results than 2D FFT, but the former needs nearly doubled computer times. Over the South China Sea, by the inverse Vening Meinesz formula and the 1D FFT we derived a set of gravity anomalies better than that from Sandwell and Smith (1997) when comparing with the shipborne gravity anomalies. Using the simulated deflections from EGM96 over the South

Table 2. Statistics of the EGM96 geoid and the differences between the predicted and the EGM96 geoids over the South China Sea (unit: m; [a]IE: innermost zone effect)

Case	mean	min.	max.	std. dev.	RMS
EGM96 deg 181 to 360	0.000	−2.998	3.812	0.542	0.542
EGM96 - 1D FFT/IE[a]	0.038	−0.010	0.100	0.014	0.041
EGM96 - 1D FFT/no IE	0.038	−0.055	0.169	0.021	0.043
EGM96 - 2D FFT	0.033	−0.060	0.169	0.019	0.038

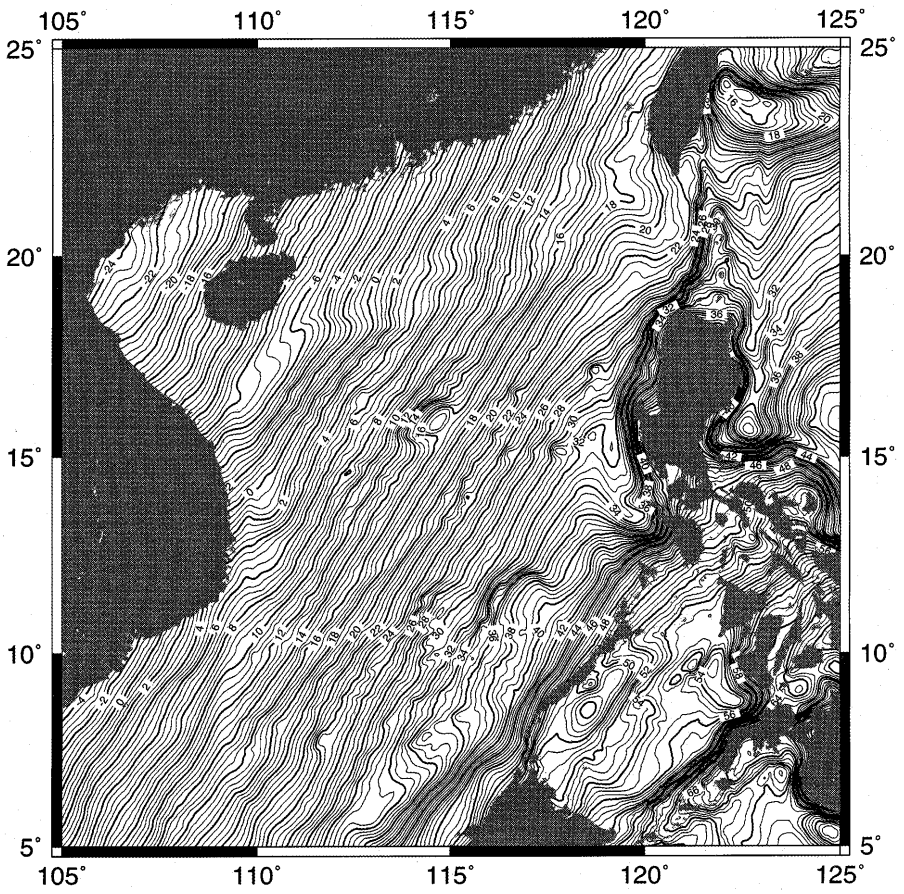

Fig. 5. The predicted geoid over the South China Sea, contour interval is 0.5 m

China Sea, the deflection-geoid formula yields a 4-cm accuracy. The predicted gravity anomalies and geoidal undulations over the South China Sea are freely available to all scientists. Interested readers please send e-mail to hwang@geodesy.cv.nctu.edu.tw.

Acknowledgements. This research is funded by the National Science Council of Republic of China, under contract NSC86- 2611-M-009-001-OS, with the project title: Surveying gravity and bathymetry over the South China Sea using satellite altimetry. The author is grateful to Roger Haagamans and an anonymous reviewer for their important suggestions.

Appendix: derivations of closed forms of *H* and *C* functions

Consider the generating function of Legendre polynomials (Hobson 1965)

$$\mathrm{f}(k) = \frac{1}{\sqrt{1 - 2k\cos\psi + k^2}} = \sum_{n=0}^{\infty} k^n P_n(\cos\psi) \tag{A1}$$

The series in Eq. (A1) is absolutely and uniformly convergent if $k < 1$ (Hotine 1969, p. 310). The case $k = 1$ will be of conditional convergence except at $\psi = 0$. In the following derivations, we exclude the point $\psi = 0$ in all results. Setting $k = 1$ in Eq. (A1), we have

$$X(\psi) = \sum_{n=0}^{\infty} P_n(\cos\psi) = \frac{1}{\sqrt{2 - 2\cos\psi}} = \frac{1}{2\sin\frac{\psi}{2}} \tag{A2}$$

Using Eq. (A1) and the fact that $P_0(\cos\psi) = 1$, we have

$$\frac{f(k) - 1}{k} = \sum_{n=1}^{\infty} k^{n-1} P_n(\cos\psi) \tag{A3}$$

Integrating Eq. (A3) with respect to k between the limits k, 0, and using the result in Gradshteyn and Ryzhik (1994, p. 101), we have

$$\begin{aligned} \sum_{n=1}^{\infty} \int_0^k k^{n-1}\mathrm{d}k P_n(\cos\psi) &= \sum_{n=1}^{\infty} \frac{1}{n} k^n P_n(\cos\psi) \\ &= \int_0^k \frac{f(k) - 1}{k}\mathrm{d}k \\ &= -\log(2\sqrt{1 - 2k\cos\psi + k^2} + 2 - 2k\cos\psi) + \log 4 \end{aligned} \tag{A4}$$

Setting $\mathrm{K} = 1$, we get

$$Y(\psi) = \sum_{n=1}^{\infty} \frac{1}{n} P_n(\cos\psi) = -\log\left[\sin\frac{\psi}{2}\left(1 + \sin\frac{\psi}{2}\right)\right] \tag{A5}$$

Furthermore, integrating Eq. (A1) with respect to k between the limits k, 0 and using the result in Gradshteyn and Ryzhik (1994, p. 99), we have

$$\begin{aligned}\sum_{n=0}^{\infty}\int_0^k k^n \mathrm{d}k P_n(\cos\psi) &= \sum_{n=0}^{\infty}\frac{1}{n+1}k^{n+1}P_n(\cos\psi)\\ &= \int_0^k \mathrm{f}(k)\mathrm{d}k\\ &= \log(2\sqrt{1-2k\cos\psi+k^2}\\ &\quad +2k-2\cos\psi)\\ &\quad -\log(2-2\cos\psi)\end{aligned} \tag{A6}$$

Setting $k=1$, we have

$$Z(\psi)=\sum_{n=0}^{\infty}\frac{1}{n+1}P_n(\cos\psi)=\log\left(\frac{1+\sin\frac{\psi}{2}}{\sin\frac{\psi}{2}}\right) \tag{A7}$$

It is easy to see that $H(\psi)$ and $C(\psi)$ are linear combinations of the three basic infinite series, $X(\psi), Y(\psi)$ and $Z(\psi)$, namely,

$$\begin{aligned}H(\psi) &= \sum_{n=2}^{\infty}\frac{(2n+1)(n-1)}{n(n+1)}P_n(\cos\psi)\\ &= \sum_{n=2}^{\infty}\left(2-\frac{1}{n}-\frac{2}{n+1}\right)P_n(\cos\psi)\\ &= 2(X(\psi)-P_0-P_1)-(Y(\psi)-P_1)\\ &\quad -2(Z(\psi)-P_0-\tfrac{1}{2}P_1)\\ &= \frac{1}{\sin\frac{\psi}{2}}+\log\left(\frac{\sin^3\frac{\psi}{2}}{1+\sin\frac{\psi}{2}}\right)\end{aligned} \tag{A8}$$

and

$$\begin{aligned}C(\psi) &= \sum_{n=2}^{\infty}\frac{2n+1}{n(n+1)}P_n(\cos\psi)\\ &= \sum_{n=2}^{\infty}\left(\frac{1}{n}+\frac{1}{n+1}\right)P_n(\cos\psi)\\ &= Y(\psi)-P_1+Z(\psi)-P_0-\tfrac{1}{2}P_1\\ &= -2\log\sin\tfrac{\psi}{2}-\tfrac{3}{2}\cos\psi-1\end{aligned} \tag{A9}$$

where $P_0=1, P_1=\cos\psi$.

References

Briaiis A, Patrait P, Tapponnier P (1993) Updated interpretation of magnetic anomalies and sea floor spreading stages in the South China Sea: implications for the Tertiary tectonics of Southeast Asia. J Geophys Res 98: 6299–6328

Courant R, Hilbert D (1953) Methods of mathematical physics, vol I. Interscience, New York

Gradshteyn IS, Ryzhik IM (1994) Table of integrals, series, and products (5th edn). Academic Press, New York

Haagmans R, de Min E, van Gelderen M (1993) Fast evaluation of convolution integrals on the sphere using 1D FFT, and a comparison with existing methods for Stokes integral. Manuscr Geod 18: 227–241

Haxby WF, Karner GD, Labreque JL, Weissel JK (1983) Digital images of combined oceanic and continental data sets and their used in tectonic studies. EOS Trans Am Geophys Un 64: 995–1004

Heiskanen WA, Moritz H (1967) Physical geodesy. Freeman WH, San Francisco

Hobson EW (1965) The theory of spherical and ellipsoidal harmonics (2nd edn). Chelsea, New York

Hotine M (1969) Mathematical geodesy. ESSA Monogr no 2, US Dept Commerce, Washington DC

Hwang C (1993) Fast algorithm for the formation of normal equations in a least-squares spherical harmonic analysis by FFT. Manuscr Geod 18: 46–52

Hwang C (1997) Analysis of some systematic errors affecting altimeter-derived geoid gradient with applications to geoid determination over Taiwan. J Geod 71: 113–130

Hwang C, Parsons B (1995) Gravity anomalies derived from Seasat, Geosat, ERS-1 and TOPEX/POSEIDON altimetry and ship gravity: a case-study over the Reykjanes Ridge. Geophys J Int 122: 511–568

Hwang C, Parsons B (1996) An optimal procedure for deriving marine gravity from multi-satellite altimetry. Geophys J Int 125: 705–718

Lemoine FG, et al. (1997) The development of the NASA GSFC and NIMA joint geopotential model. In: Segawa J, Fwimoto H (eds) Proc Int Symp Gravity, geoid, and marine geodesy

Levitus S (1982) Climatological atlas of the world ocean. NOAA professional paper 13, US Dept Commerce. Rockville, Md

Meissl P (1971) A study of covariance functions related to the earth's disturbing potential. Rep no 151, Dept Geod Surv, Ohio State University, Columbus

Mesko AM (1984) Digital filtering: applications in geophysical exploration for oil. Akademiai Kiado, Budapest

Molodenskii MS, Eremeev VF, Yurkina MI (1962) Methods for study of the external gravitational field and figure of the earth. Works of Central Research Institute of Geodesy, Aerial Photography and Cartography, no 131, Moscow

Olgiati A, Balmino G, Sarrailh M, Green CM (1995) Gravity anomalies from satellite altimetry: comparison between computation via geoid heights and via deflections of the vertical. Bull Geod 69: 252–260

Rummel R, van Gelderen M (1995) Meissl scheme – spectral characteristics of physical geodesy. Manuscr Geod 20: 379–385

Sandwell D, Smith WHF (1997) Marine gravity anomaly from Geosat and ERS-1 satellite altimetry. J Geophys Res 102: 10039–10054

Schwarz KP, Sideris MG, Forsberg R (1990) The use of FFT techniques in physical geodesy. Geophys J Int 100: 485–514

Tziavos IN (1996) Comparisons of spectral techniques for geoid computations over large regions. Manuscr Geod 70: 357–373

Vening Meinesz FA (1928) A formula expressing the deflection of the plumb-line in the gravity anomalies and some formulae for gravity field and the gravity potential outside the geoid. Proc Koninkl Ned Akad Wettenschap. vol 31